The α_s Measurement from Jet Rates in Deep Inelastic ep Scattering at HERA

Richard Nisius [1]
I. Physikalisches Institut RWTH Aachen
Sommerfeldstr.
D 52056 Aachen, Germany

Abstract: The measurement of the strong coupling constant α_s based on jet rates in deep inelastic ep scattering at HERA is discussed. The determination from the H1 experiment in next to leading order results in $\alpha_s(M_z^2) = 0.123 \pm 0.018$.

[1]Representing the H1 and ZEUS Collaborations. Supported by the BMFT

1 Introduction

Neutral current deep inelastic electron proton scattering (DIS) is investigated using data from the 1993 run of the HERA ep collider at DESY. This scattering can be written as $e(k)\, p(P) \to e'(k')\, X(h)$, where the symbols in brackets denote the particle four vectors. It is sketched in figure 1, which also introduces the basic kinematic quantities used later on.

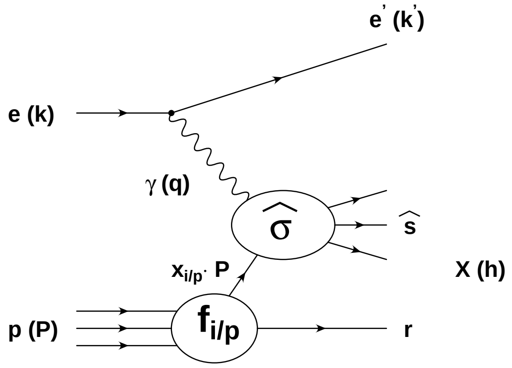

Figure 1: *A sketch of neutral current deep inelastic ep scattering.*

At HERA, electrons of 26.7 GeV momentum are scattered off protons of 820 GeV momentum leading to a center of mass energy of 296 GeV. In the deep inelastic scattering regime, momentum transfers squared Q^2 in the range $10 < Q^2 < 4000\ GeV^2$, $(Q^2 = -q^2)$ are considered at present. The two experiments H1 [1] and ZEUS [2] allow to observe the scattered electron (e') and also the hadronic final state (X), the main interest of the analysis discussed here.

In lowest order, neutral current DIS jet production can be described as purely electromagnetic scattering of the electron off a quark via single photon exchange. In the Q^2 range studied, the exchange of the intermediate vector boson Z° is highly suppressed due to it's large mass. This scattering leads to (1+1) jet events. One jet is caused by the scattered quark (1), the other by the leftover part of the proton (+1), which is only partially observed in the detectors.

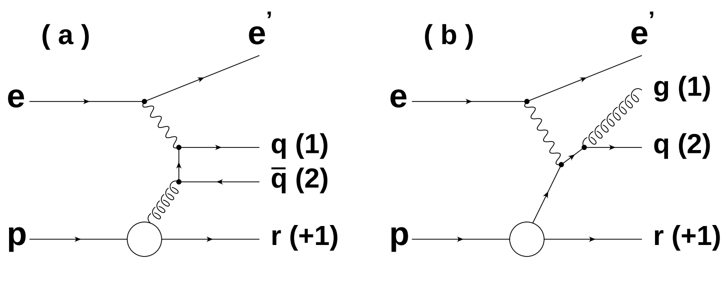

Figure 2: *Generic Feynman diagrams of the LO contributions to (2+1) jet events.*

Higher jet multiplicities are described in the framework of QCD. The corresponding cross sections are expressed as power series in α_s, such that the leading order (LO) contribution to (2+1) jet events is at $\mathcal{O}(\alpha_s)$. Two generic graphs contribute (see figure 2). As both diagrams contain couplings to gluons it is clear that (2+1) jet production is sensitive to α_s.

2 Jet rates compared to theoretical predictions

At HERA the fractional (2+1) jet rate is chosen [3] to explore the running of $\alpha_s(\mu^2)$ as function of the varying momentum transfer squared Q^2, which is identified with the renormalization scale ($Q^2 = \mu^2$).

This method allows to study the evolution of $\alpha_s(Q^2)$ over a wide range of Q^2 by using only one observable in a single experiment. The lowest reachable Q^2 is given by the lower cutoff in Q^2 at which perturbative QCD is considered as an applicable theory, and the upper cutoff in Q^2 is the center of mass energy squared of the collider.

The fractional (2+1) jet rate is defined for each bin in Q^2 as:

$$R_{2+1}(Q^2, y_c) = \frac{\sigma_{2+1}(Q^2, y_c)}{\sigma(Q^2)} \tag{1}$$

Here $\sigma(Q^2)$ represents the sum of (1+1) and (2+1) jet cross sections. The jet resolution parameter y_c is defined as $y_c = m_{ij}^2/W^2$, where m_{ij}^2 is the invariant mass squared of two objects i, j and W is the invariant mass of the hadronic system. This rate is known theoretically in next to leading order (NLO), that means up to $\mathcal{O}(\alpha_s^2)$ [4].

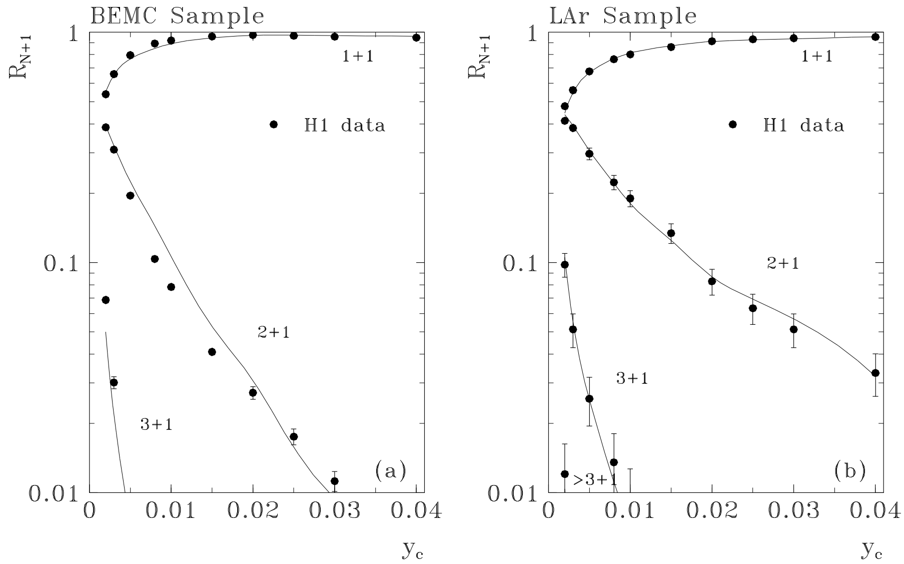

Figure 3: *Fractional jet rates as obtained by H1 in the kinematic domains discussed in the text, compared to LEPTO6.1 (MEPS) (full lines), for (a) $Q^2 < 100$ GeV^2, (b) $Q^2 > 100$ GeV^2. Only statistical errors are shown.*

As demanded by the theoretical calculations available in the PROJET [5] and DISJET [6] Monte Carlos, jets are experimentally reconstructed using a modified JADE [7] algorithm with W^2 as the mass scale. This algorithm takes into account the invisible part of the proton remnant, by including a pseudo particle in the clustering procedure representing the missing longitudinal momentum in the event [8]. As the calculation is done for massless partons in NLO it does not perform combinations of massive objects while defining the jets, which makes this Lorentz invariant result as well recombination scheme independent. Therefore the frame of reference in which the experimental jet clustering is performed and the recombination scheme used in the jet algorithm is a free choice of the experiments. In this analysis jet counting is done in the laboratory frame using the JADE recombination scheme, as this combination gives the best correlation of the partonic jet rates and the jet rates obtained at the detector level from reconstructed calorimetric energy deposits [3].

The $\mathcal{O}(\alpha_s^2)$ calculations are only available as parton level jet cross section Monte Carlos and not as event generators. This implies, that the relation between observed jets in the detector and the underlying partonic jet configuration has to be obtained from the available LO event generators. For this purpose LEPTO6.1 [9] is used. Events can be generated using the LO matrix elements alone,

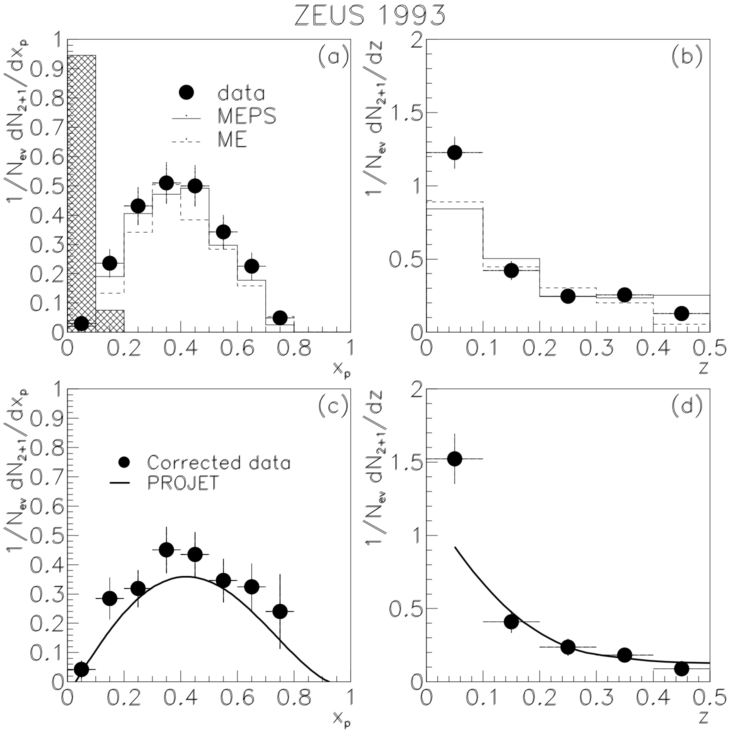

Figure 4: *The x_p and z distributions as obtained by ZEUS in the kinematic domain* $160 < Q^2 < 1280$ GeV^2 *and* $0.01 < x < 0.1$. *The uncorrected distributions are compared to the predictions of LEPTO6.1 (a,b). Using MEPS the data are corrected to the level of parton jets and compared to the PROJET calculation (c,d). The shaded histogram shows the x_p distribution for a low Q^2 control sample. The z distribution is symmetric to $z = 0.5$ by construction.*

referred to as (ME), or by matching leading log parton showers to these matrix elements in order to account for a part of the higher order terms (MEPS).

Figure 3 shows the fractional jet rates, at the level of detector jets, as measured by H1 [10] compared to MEPS in the phase space regions defined in section 3. For $Q^2 > 100$ GeV^2, figure 3b, the description of the observed jet rates by MEPS is excellent, whereas for $Q^2 < 100$ GeV^2, figure 3a, the description is acceptable only for $y_c \geq 0.02$. A crucial point of this comparison is the restriction of phase space for the jets. Events count as (2+1) jets only if both jets are observed in the angular region $10^\circ < \vartheta_{jet} < 145^\circ$. All polar angles are calculated with respect to the momentum vector of the incoming proton. Especially the region of small ϑ_{jet} is critical as it contains jets from the initial state parton shower and in addition products from the not well understood proton remnant fragmentation. In this region the experiments observe more jets than predicted by LEPTO6.1 and the NLO calculation respectively. The good description of the data by LEPTO6.1 for $y_c \geq 0.02$ allows to use it to correct the data to the level of parton jets. These can be compared to the NLO calculation.

Figure 4 shows the distribution of the scaling variables x_p and z $(0 \leq x_p, z \leq 1)$ defined as

$$x_p = \frac{x}{x_{i/p}} = \frac{Q^2}{Q^2 + \hat{s}} \qquad\qquad z = \frac{P \cdot p_{jet}}{P \cdot q} = \frac{1}{2}\,(1 - \cos\vartheta^\star_{jet}) \tag{2}$$

and measured by ZEUS [11]. Here $\vartheta^\star_{jet}$ denotes the jet scattering angle in the photon parton center of mass system. The data are compared to LEPTO6.1 and PROJET [2]. The scaling variables are calculated assuming massless jets in the laboratory frame. The uncorrected distributions normalized

[2]This older version of the program used by ZEUS does not contain the contribution of the $\mathcal{O}(\alpha_s^2)$ terms for (2+1) jet events stemming from virtual photons with longitudinal polarization, which however is proven to be a very small effect.

to the total number of events are compared to ME and MEPS predictions. The x_p distribution, figure 4a, is reproduced by the Monte Carlo and it shows the need of including the parton showers which give a larger number of (2+1) jet events over the whole range. The z distribution, figure 4b, is well described except for the lowest z bin, which corresponds to forward scattering in the photon parton center of mass frame. The ZEUS data corrected bin by bin using the MEPS model are compared to PROJET, which predicts less (2+1) jet events in the whole x_p range but concentrated in the low z region (figure 4d). As the z distribution is flat in x_p for low z values [11] the x_p distribution would probably be well described after demanding $z > 0.1$. In conclusion, it is clear that after excluding the difficult part of low angle jet phase space a determination of α_s is possible.

3 Determination of α_s

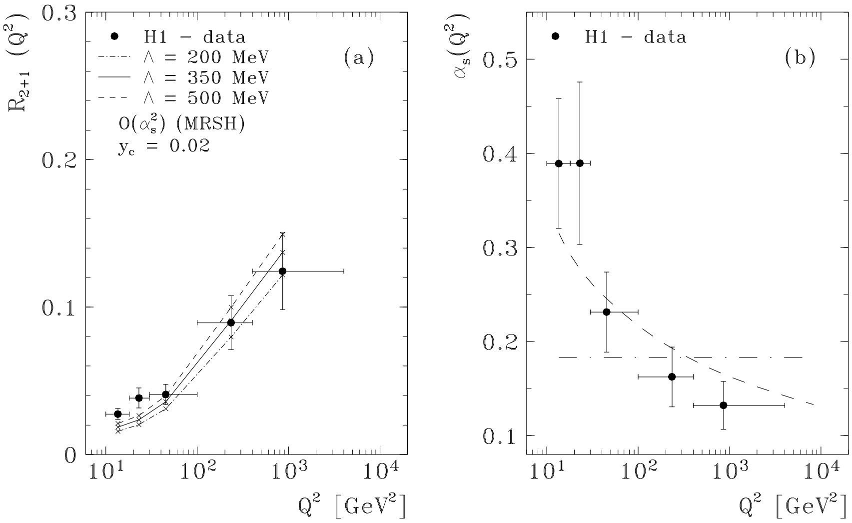

Figure 5: *The α_s measurement for $y_c = 0.02$ from H1 using the MRSH parton density parametrizations. (a) The corrected jet rate $R_{2+1}(Q^2, y_c)$ and the PROJET predictions, (b) the derived α_s values, both as function of Q^2. Only statistical errors from the data and the correction factors are shown.*

In order to compare the measured jet rates to the NLO calculation it is necessary to apply to the NLO Monte Carlo the same phase space restrictions in terms of electron variables and jet quantities as done in an experimental event selection, otherwise the extrapolation to the full phase space would lead to large uncertainties. The PROJET Monte Carlo was adapted to provide this feature.

The H1 event selection requires $W^2 > 5000\ GeV^2$ and an electron candidate fulfilling $160° < \vartheta_e < 172.5°$, $10 < Q^2 < 100\ GeV^2$ and $E_e > 14\ GeV$, **or** an electron candidate with $10° < \vartheta_e < 148°$, and $Q^2 > 100\ GeV^2$ and $y < 0.7$. Here E_e and ϑ_e are the energy and angle of the scattered electron, and y is the Bjorken scaling variable.

Figure 5a compares the H1 measurement of $R_{2+1}(Q^2, y_c = 0.02)$, corrected to the level of parton jets using MEPS, to the NLO calculation from PROJET for various $\Lambda_{4,\overline{MS}}$ values assuming that the set MRSH [12] represents the correct parton density parametrizations (PDFs). This is translated into five measurements of $\alpha_s(Q^2)$ and fitted to the 2-loop solution of the renormalization group equation (falling curve), and to the assumption of a constant α_s (horizontal line) shown in figure 5b. The running of $\alpha_s(Q^2)$ is preferred by the data.

The systematic uncertainty of the procedure to correct the observed jet rate to the parton jet rate, which is important especially at low Q^2, is studied by using the CDM [13] model to obtain the correction factors [10], which leads to much larger values of α_s for low Q^2. Therefore at this stage the α_s determination is restricted to $Q^2 > 100\ GeV^2$ where the correction factors obtained from both models converge.

The fitted value $\alpha_s(M_Z^2) = 0.123 \pm 0.012_{stat} \pm 0.013_{sys}$ [10] is consistent with the world average [14, 15]. The systematic error covers the variation of the jet angle cuts, the uncertainty of the measurement of hadronic energies, the y_c dependence, the effects of different PDF's, the variation of the renormalization and factorization scales and the model dependence of the correction procedure.

One particular point of interest is the correlation of the measured value of α_s in this analysis with the value determined while fitting the PDFs which is then used for evolving the PDFs [3, 16]. This was studied using the GRV94 PDFs which are available for various $\Lambda_{4,\overline{MS}}$ values [17] in the range $0.15 - 0.35\ GeV$. Although $\alpha_s(M_Z^2)$ used in the PDFs changes by 0.015, the fitted value only differs by 0.003, which at this point is a negligible error.

4 Conclusions and outlook

Jet rates in neutral current deep inelastic *ep* scattering at HERA are used to extract the strong coupling constant α_s in NLO, leading to an H1 measurement of $\alpha_s(M_Z^2) = 0.123 \pm 0.018$. This value is consistent with other experiments. In future, with higher statistics and better understanding of the systematic error, the measurement will be improved considerably.

References

[1] H1 Collaboration, (I. Abt, et al.), DESY 93-103.

[2] ZEUS Collaboration, (M. Derrick, et al.), Phys. Lett. **B293**, 465 (1992);
The ZEUS Detector, status report 1993, DESY 1993.

[3] R. Nisius, PhD thesis, Aachen preprint PITHA 94/21 (1994).

[4] D. Graudenz, Phys. Lett. **B256**, 518 (1991); D. Graudenz, Phys. Rev. **D49**, 3291 (1994); J.G. Körner, E. Mirkes, G.A. Schuler, Int. J. Mod. Physics **A4**, 1781 (1989); T. Brodkorb, J.G. Körner, Z. Phys. **C54**, 519 (1992).

[5] D. Graudenz, PROJET4.1, CERN-TH.7420/94 (The latest version); PROJET4.0 unpub. (The version used by H1); PROJET3.6 unpub. (The version used by ZEUS).

[6] T. Brodkorb, E. Mirkes, DISJET manual, Univ. of Wisconsin, MAD/PH/821 (1994);
T. Brodkorb, E. Mirkes, Univ. of Wisconsin, MAD/PH/820 (1994).

[7] JADE Collaboration, (W. Bartel, et al.), Z. Phys. **C33**, 23 (1986).

[8] D. Graudenz, N. Magnussen, Proc. Workshop 'Physics at HERA', DESY, Hamburg, Vol. 1, 261 (1991), and contributions therein.

[9] G. Ingelman, "LEPTO 6.1", Proc. Workshop 'Physics at HERA', DESY, Hamburg, Vol. 3, 1366 (1991).

[10] H1 Collaboration (T. Ahmed, et al.), Phys. Lett. **B346**, 415 (1995).

[11] ZEUS Collaboration, (M. Derrick, et al.), DESY-95-016, accepted by Z. Phys. **C** .

[12] A.D. Martin, W.J. Stirling, R.G. Roberts, Proc. of the Workshop on Quantum Field theory and Theoretical Aspects of High Energy Physics, eds. B. Geyer and E.M. Ilgenfritz, 11 (1993).

[13] L. Lönnblad, ARIADNE4.03, Comput. Phys. Commun. **71**, 15 (1992), and references therein.

[14] Particle Data Group, (L. Montanet, et al.), Phys. Rev. **D50**, 1297 (1994).

[15] S. Bethke, these proceedings.

[16] B.R. Webber, Cavendish-HEP-94/15.

[17] A. Vogt, private communication, DESY-95-068.